Nucleic Acids Research, 1999, Vol. 27, No. 24 **4715–4724**

The *top3*$^+$ gene is essential in *Schizosaccharomyces pombe* and the lethality associated with its loss is caused by Rad12 helicase activity

Mohamed Maftahi[1], Christine S. Han[1], Lance D. Langston[1], Justin C. Hope[2], Nico Zigouras[1] and Greg A. Freyer[1,2,*]

[1]Division of Environmental Sciences, Joseph Mailman School of Public Health and [2]Department of Anatomy and Cell Biology, College of Physicians and Surgeons, Columbia University, New York, NY 10032, USA

Received September 1, 1999; Revised and Accepted October 26, 1999

DDBJ/EMBL/GenBank accession no. AF126287

ABSTRACT

The topoisomerase III gene (*top3*$^+$) from *Schizosaccharomyces pombe* was isolated and a targeted gene disruption (*top3*::*kan*^{R}) was used to make a diploid strain heterozygous for *top3*$^+$. The diploid was sporulated and the *top3*::*kan*^{R} spores went through four to eight cell divisions before arresting as elongated, predominantly binucleated cells with incompletely segregated chromosomes. This demonstrates that *top3*$^+$ is essential for vegetative growth in fission yeast. The aberrant chromosomal segregation seen in *top3*::*kan*^{R} cells is unlike the 'cut' phenotype seen in mitosis-defective mutants and so we refer to this phenotype as 'torn'. A deletion mutant, *rad12-hd* (*rad12* is a homolog of *Saccharomyces cerevisiae SGS1*), partially suppressed the lethality of *top3* mutants. A point mutant, *rad12-K547I*, which presumably eliminates helicase activity, also suppresses the lethality of *top3* mutants, demonstrating that the lethality seen in *top3*$^-$ cells is most likely caused by the helicase activity of Rad12. This double mutant grows very slowly and has much lower viability compared to *rad12-hd top3*::*kan*^{R} cells, implying that the helicase activity of Rad12 is not the only cause of *top3*$^-$ lethality. The low viability of *rad12*$^-$ *top3*$^-$ mutants compared with *rad12* single mutants suggests that Top3 also functions independently of Rad12.

INTRODUCTION

The exact role of topoisomerase III (Topo III) in cells is not completely understood. Originally discovered in bacteria, it has now been shown to exist in other organisms, including humans and mice (1,2). In *Escherichia coli*, Topo III has been shown to possess potent decatenating activity, particularly when single-stranded (ss)DNA is present in the molecules (3). *Escherichia coli* Topo III removes negative supercoils, an activity that also requires ssDNA in the substrate (3). More recently it was shown that *E.coli* RecQ helicase activity stimulates Topo III to fully catenate plasmid DNA (4). RecQ helicase was shown to bind closed circular DNA, presumably creating a single-stranded region for Topo III to catenate double-stranded (ds)DNA molecules. The presence of a single-stranded region in the DNA substrate was not sufficient to stimulate catenation by Topo III, supporting a specific requirement for RecQ helicase in this reaction (4).

Eukaryotic Topo III is a type I topoisomerase and a member of the *E.coli* type I topoisomerase family, which includes *E.coli* topoisomerases I and III (1,5–7). The first description of Topo III in eukaryotic cells came from a screen of hyper-recombination mutants in *Saccharomyces cerevisiae* (7). A mutant was isolated that showed hyper-recombination as well as slow growth. In addition, this mutant was found to be sterile. Isolation of the gene revealed that it shared homology with the *E.coli topA* and *topB* genes (the genes coding for topoisomerases I and III, respectively). This homology was confirmed by the ability of the bacterial *topA* gene to complement the slow growth phenotype of the yeast mutant (7). These data, along with the finding that the gene shared no homology with other eukaryotic topoisomerase genes, led the authors to name it *TOP3*. *In vitro*, the *TOP3* gene product was shown to weakly relax negatively but not positively supercoiled DNA (5). These investigators also observed that Topo III has a strong preference for binding to ssDNA and that it is a relatively weak topoisomerase. Their studies also considered the activities of *E.coli* topoisomerases I and III and concluded that biochemically it is more similar to bacterial Topo III. In mice, Topo III is widely expressed in several tissues (2,8). Extremely high levels of Topo III mRNA were detected in mouse testis beginning some 12–14 days after birth. Knockout mice die as embryos, suggesting that Topo III is an essential gene in early mouse development (6).

A screen for extragenic suppressors of the *top3* mutant phenotype in *S.cerevisiae* led to isolation of a gene designated *SGS1*, for slow growth suppressor (9). Two-hybrid studies showed that the gene product of *SGS1* interacts with both

*To whom correspondence should be addressed at: P.I. Annex Room 114, 722 West 168th Street, Columbia University, New York, NY 10032, USA. Tel: +1 212 543 4124; Fax: +1 212 781 4993; Email: gaf1@columbia.edu

Table 1. *Schizosaccharomyces pombe* strains used in this study

Strain (laboratory) name	Genotype
972 (SZ06)	h^{-S}
rad12::*hd* (SZ36)	h^{-S}, *ade6-210, leu1-32, ura4-D18, rad12*::*ura4*$^{+}$
top3^{+}/*top3*::*kan*^{R} (SZ107)	$h^{+N}h^{-S}$ *ura4-D18/ura4-D18, leu1-32/leu1-32, adeM210/adeM216, top3*::*kmx*$^{+}$/*top3*$^{+}$
rad12-hd top3::*kan*^{R} (SZ109)	h^{-S}, *ade6-210, leu1-32, ura4-D18, rad12*::*ura4*$^{+}$, *top3*::*kmx*$^{+}$
FC584 (SZ106)	$h^{+N}h^{-S}$ *ura4/ura4, leu1-32/leu1-32, adeM210/adeM216*
rad12-K547I (SZ123)	h^{-S}, *ade6-210, leu1-32, ura4-D18, rad12-K547I*
rad12-K547I top3::*kan*^{R} (SZ124)	h^{-S}, *ade6-210, leu1-32, ura4-D18, rad12-K547I, top3*::*kmx*$^{+}$

All the strains are isogenic to 972, except the SZ109 diploid strain, which was used in the *top3*$^{+}$ disruption experiment.

topoisomerases II and III (9,10). Sgs1 was shown to be a helicase of the RecQ family (9,10). In *E.coli*, loss of RecQ helicase has been associated with increased illegitimate recombination (11). In association with other mutations, RecQ mutants are UV sensitive and have greatly reduced homologous recombination (12,13). Sgs1 is three times the size of RecQ, possessing additional sequences both N- and C-terminal to the centrally located helicase. This family has since been expanded to include the human *BLM* and *WRN* genes (associated with Bloom's and Werner's syndromes, respectively), human *RECQ* (*hRECQ*) and two other recently identified human genes containing recQ helicase domains (14–19). The physical association between Topo III and Sgs1 suggests a functional relationship between these two proteins, where Sgs1 creates products whose resolution depends on Topo III. This suggestion is based on the fact that the slow growth seen in Top3-deficient cells is suppressed by loss of the Sgs1 helicase.

In the fission yeast *Schizosaccharomyces pombe*, the *rad12*$^{+}$ gene (also referred to as *rqh1*$^{+}$ and *hus2*$^{+}$) has been isolated and shown to be another member of the RecQ helicase family (20,21). This gene was initially identified in a screen for radiation-sensitive mutants (22) and was independently isolated as *hus2*$^{+}$ in a screen for hydroxyurea (HU)-sensitive mutations (23). Our interest in *rad12*$^{+}$ began with the finding that the *rad12-502* mutant has reduced levels of Uve1 activity, a UV damage endonuclease (24). *rad12*$^{-}$ cells are UV- and γ-radiation-sensitive as well as sensitive to HU (20,21,23). In addition, *rad12* mutants show chromosomal instability and demonstrate a defect in exiting a HU-induced checkpoint (20,21). This defect was manifested in cells as missegregated chromosomes where DNA is seen stretching between paired nuclei in elongated cells. Because of the relationship of Sgs1 and Top3, we sought to understand whether a similar association existed between Rad12 and Top3 in *S.pombe*. Here we describe the isolation of *S.pombe top3*$^{+}$ and show that it is essential. Interestingly, the phenotype that we observe in *top3*::*kan*^{R} cells is reminiscent of the chromosomal missegregation seen in *rad12*$^{-}$ cells upon exit from S phase checkpoint arrest. To distinguish this phenotype from 'cut', where the septum splits the nucleus, we suggest the term 'torn' to describe this phenotype, referring to the ripped appearance of the chromosomes and the absence of an obvious septum in these cells. We further show that the lethality of *top3*::*kan*^{R} cells is suppressed in *rad12* mutants and present evidence that the lethality is partially dependent on Rad12 helicase activity, although helicase activity alone may not fully explain the lethality. Finally, *rad12* mutants do not completely restore viability in *top3* mutants, demonstrating that Top3 may also function independently of Rad12.

MATERIALS AND METHODS

Media and strains

Media. The sporulation medium was EMM with no nitrogen, supplemented as appropriate. YEA was 30 g/l glucose, 5 g/l yeast extract and 75 mg/l adenine. Minimal medium was 1.7 g of yeast nitrogen base (Bufferad) and 5 g $(NH_4)_2SO_4$, supplemented with 75 μg/ml uracil, 75 μg/ml leucine and 75 μg/ml adenine unless indicated otherwise.

Strains. All strains used in this study are shown in Table 1.

Plasmids and strain constructions

Cloning of S.pombe top3^{+} *cDNA.* A partial cDNA for *top3*$^{+}$ was isolated by PCR amplification of a 292 bp fragment using degenerate primers (Top3sp5′ and Top3sp3′) based on two highly conserved sequences in the *S.cerevisiae* and human *TOP3* genes. (All oligonucleotides used in this study are shown in Table 2.) The template was 1 μg of plasmid DNA isolated from a *S.pombe* cDNA library. The PCR product was sequenced and the results used to search the *S.pombe* genome database at the Sanger Center. This search identified a cosmid (c16g5) containing a probable *top3* gene. Likely exons and intron boundaries were identified by comparing the open reading frames from this cosmid with the sequence of *S.cerevisiae TOP3.*

To isolate a full-length cDNA, 1 μg of a *S.pombe* cDNA library was used as template for PCR amplification using *Pfu* polymerase (Stratagene) and primers (cTOPA and cTOPD) predicted to bracket the complete coding region of *top3*$^{+}$. The products were gel purified, digested with *Nco*I and *Sal*I, and cloned into pBluescript (Stratagene). The resulting cDNA, designated pMM1, was completely sequenced using oligonucleotide primers, whose sequences were based on the genomic sequence.

top3^{+} *genomic clone.* A library made by partial *Hin*dIII digestion of *S.pombe* genomic DNA was screened with a radiolabeled probe for clones containing *top3*$^{+}$ sequences. A plasmid (pgTOP3) identified in this screen was shown to contain the entire *top3*$^{+}$ gene by restriction analysis and by PCR amplification of the 5′-end, middle and 3′-end of the gene

Table 2. Oligonucleotides used in this study

Oligonucleotide	Sequence	Purpose
Top3sp5′[a]	TGCCAGTTYCCHACNCTBGGCTTTG[b]	Degenerate oligo used to isolate *top3*$^+$
Top3sp3′[a]	CTGTTCKWGGATAAGAWATRAAMCC[c]	Degenerate oligo used to isolate *top3*$^+$
cTOPA[d]	AAGGCAGTCCATGGCTATGCGCGTCCTATGTGTTGCTG	Primes at 5′ ATG of *top3*+ to make full-length cDNA
cTOPD[d]	CCGCGAAGTCGACCTAGGTTTGCGGTTCATTATGAC	Primes at 3′ stop of *top3*$^+$ to make full-length cDNA
cTOP1[d]	ATGCGCGTCCTATGTGTTGC	Verify genomic clone
cTOP3[d]	GTGATGATTTGAGCATCG	Verify genomic clone
cTOP11[d]	CGGGACAGATGCTACTATG	Verify genomic clone
TOP3ver2	ACGGATCCAACTCAAGATG	Verify genomic clone and TOP3 disruption
cTOP9[d]	CCAAAGGAGCCGAAACG	Verify genomic clone
cTOP13[d]	GGATCATATGAACTAGAAC	Verify genomic clone
top3cNotI	ACGAGGCAGCGGCCGCGACGCTTAAAAACGAAAG	Create *top3*$^+$ disruption
top3dSpeI	CGATGCACACTAGTGGCTTCCGTAATAA	Create *top3*$^+$ disruption
top3e	GGTTAATCGCACCTCC	Create *top3*$^+$ disruption
top3f	CTTGGATATTGCACACC	Create *top3*$^+$ disruption
TOP3ver1	CGGCTGCAAGGTCTTCGTC	Verify *top3*$^+$ disruption
Kan1	GCGGCGTGGGGACAATTC	Verify *top3*$^+$ disruption
KanRev	CCTCGACATCATCTGCCC	Verify *top3*$^+$ disruption

[a]The degenerate oligonucleotides were designed using the codon bias of *S.pombe*.
[b]y = c + t; h = a + c + t; n = a + c + t + g; b = c + t + g.
[c]w = a + t; r = a + g; m = a + c.
[d]These oligonucleotides were designed using the *top3* cDNA sequence.

using paired primers cTOP1/cTOP3, cTOP11/TOP3ver2 and cTOP9/cTOP13, respectively. pgTOP3 was further digested with *Bam*HI to eliminate sequences downstream of the gene, creating pgTOP3b. Restriction analysis showed that pgTOP3b contains 316 bp of genomic sequence upstream of the ATG start codon and 123 bp downstream from the TAG stop codon.

Construction of the top3 disrupted strains

The *top3*$^+$ gene was disrupted with the kanamycin resistance gene under the control of the TEF promoter (25). The 3′-sequences of the *top3*$^+$ gene, from nucleotide 1298 to 2261, were PCR amplified using primers top3cNotI and top3dSpeI. This 963 bp fragment was subcloned into the *Sma*I site of pBluescript, amplified, cut from there with *Eco*RI/*Spe*I (as a 618 bp fragment as there is an internal *Eco*RI site at nucleotide 1643) and cloned into the *Eco*RI and *Spe*I sites downstream of the *kan*^{r} gene in plasmid pFA-kanMX4, creating pkanMX4-top3.3′ (25). This plasmid contains the *E.coli* transposon Tn*903 kan*^{r} fused to the transcriptional and translational control sequences of the TEF gene of the fungus *Ashbya gossypii*. The 5′-upstream region of *top3*$^+$, from –951 to –25, was PCR amplified using primers top3e and top3f. This 933 bp fragment was cloned into the *Sma*I site of pBluescript, amplified, then excised from there with *Bam*HI/*Sal*I and cloned into the *Bgl*II and *Sal*I sites upstream of the *kan*^{R} gene in pkanMX4-top3.3′. The final construct was designated pTop3Kmx.

The disruption cassette was cut from pTop3Kmx with *Not*I and was used to transform the diploid strain FC584 (F. Chang) as described (26). Positive colonies were selected for on rich medium containing Geneticin (G418; Gibco). Several colonies were isolated. Proper disruption of *top3*$^+$ was confirmed by PCR. The 5′-junction was confirmed using primers TOP3ver1 and Kan1 and the 3′-junction was confirmed using primers TOP3ver2 and KanRev. The diploid strain was allowed to sporulate by streaking onto sporulation medium. Tetrads were dissected on YEA plates.

The *rad12-hd top3*::*kan*^{R} and *rad12-K547I top3*::*kan*^{R} double mutants were made by transforming *rad12-hd* and *rad12-K547I*, respectively, with *Not*I-digested pTop3Kmx. Transformants were selected for on rich medium in the presence of G418. Confirmation of the disruption was carried out by PCR analysis.

Growth kinetics

Overnight cultures grown in rich medium were diluted ~1:1000 and allowed to grow at 30°C for ~14 h. The experiment was started when there were ~2×10^5 cells/ml. Beginning at time 0 and then at each hour for the next 8 h, 100 µl of cells was placed in 1 ml of isotonic solution and counted in a Coulter counter. The particle size cut-off was set at 6 µm. Each time point was counted three times. Fold increase was calculated as relative to the first time point, time 0. Plots are averages of three independent experiments.

Photographs of mutant cells

Diploid *top3*::*kan*^{R} were plated on sporulation plates and incubated for 48 h at 30°C. Asci were scraped from the plates and resuspended in 1 ml sterile water with 5 µl glusulase. Following incubation for 8 h at 30°C, spores were plated onto rich medium plates and incubated for 36 or 72 h at 30°C. At 36 h a mixture of *top3*$^+$ and *top3*::*kan*^{R} colonies were scraped from the plates and resuspended in water, fixed in ethanol and stained with DAPI at 0.25 µg/µl. At 72 h microcolonies, assumed to be *top3*::*kan*^{R}, were plucked from the plates, fixed and stained with DAPI. All of the *rad12* single mutant and *rad12 top3* double mutant strains were also examined by

fluorescence microscopy following DAPI staining. Cells were prepared from cultures grown to mid-log.

RESULTS

Identifying *S.pombe top3*$^+$

To isolate the gene for *top3*$^+$ in *S.pombe*, we first used degenerate oligonucleotides as primers (Top3sp5′ and Top3sp3′) to PCR amplify a fragment of *top3*$^+$ using a cDNA library as the template. The oligonucleotide sequences were based on two highly conserved amino acid sequences in the human and *S.cerevisiae TOP3* genes. We then sequenced the products of these PCR reactions and used the sequences to search the *S.pombe* genome database at the Sanger Centre. This search identified a cosmid, c16G5 (GenBank accession no. AL023554) from chromosome II, which contained a probable *S.pombe top3*$^+$ homolog. Using the genomic sequence data, we developed primers to amplify a full-length *top3*$^+$ cDNA using plasmid DNA generated from a cDNA library as template. The cDNA was fully sequenced and the data compared with the genomic sequence to check for fidelity. The coding sequence (GenBank accession no. AAD22485) was used to identify the five introns in *top3*$^+$ (Fig. 1).

The complete genomic sequence of *top3*$^+$ from ATG to the stop codon is 2203 bp and the complete coding sequence (including the stop) is 1869 bp, which translates to a predicted protein of 622 amino acids of ~71.2 kDa. BLAST searches of the GenBank database reveal that *S.pombe* Top3 shares significant sequence homology with topoisomerases in organisms ranging from bacteria to humans (Table 3). An alignment of *S.pombe* Top3 with human and *S.cerevisiae* is also shown in Figure 1. Note that the human protein is larger, with 30 additional amino acids at the N-terminus and extending 350 amino acids longer at the C-terminus.

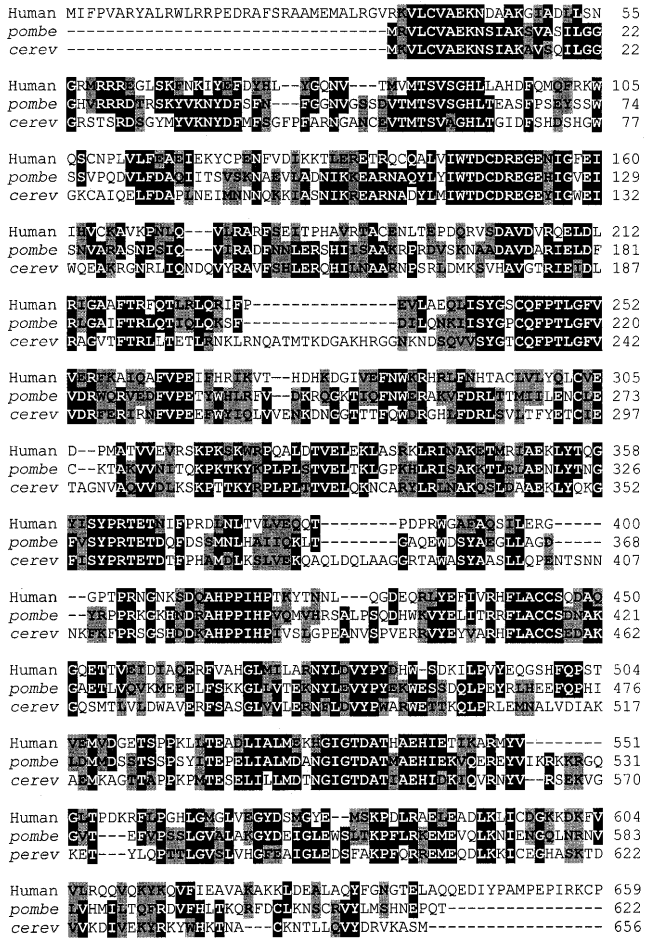

Figure 1. Comparison of the fission yeast, human and *S.cerevisiae* Top3 amino acid sequences. *Schizosaccharomyces pombe* Top3 is 622 amino acids long, comparable to the length of *S.cerevisiae* topo III, which contains 656 amino acids. While both share significant homology with human topo III, the human protein is 1001 amino acids long. Black boxes show areas of identity and gray boxes are areas of similarity.

Dissecting *top3*$^+$ function

To investigate the role of Top3 in *S.pombe* cells, we created a *top3* null mutant. We began by disrupting *top3*$^+$ with a selectable marker, *kan*^{R}, the gene for kanamycin resistance, under control of the TEF promoter (25). The disruption construct, designed to put *kan*^{R} in place of nucleotides –25 to 1643 of genomic *top3*$^+$ (Fig. 2A), was used to transform *S.pombe* diploid strain FC584. Transformants (designated *top3*$^+$/*top3*::*kan*^{R}) were selected for on rich medium containing G418 and specific integration of the *kan*^{R} marker at the *top3*$^+$ locus was confirmed by PCR.

The heterozygous diploid was allowed to sporulate and tetrad analysis showed 2:0 segregation (Fig. 2B). In this picture, four out of 12 tetrads give only one colony. This result was seen in several experiments, showing reduced spore viability in the *top3*$^+$/*top3*::*kan*^{R} diploid heterozygote. Microscopic examination of the spores which failed to form colonies showed that the cells stopped dividing after approximately four to eight cell divisions, indicating that *top3*$^+$ is essential for vegetative growth in *S.pombe*. To better understand the cause of cell death in *top3*$^-$ cells, DAPI stained cells were examined by fluorescence microscopy. The *top3*$^+$/*top3*::*kan*^{R} diploid strain was sporulated and treated with glusulase to release individual spores. To see early events, cells were scraped from plates that had been incubated for 36 h. This mixture of *top3*$^+$ and *top3*::*kan*^{R} cells was examined by fluorescence microscopy. Many cells appeared to be unable to properly segregate their chromosomes (Fig. 3B–D). These cells were elongated and often binucleated and sometimes had DAPI stained material strung out between the paired nuclei. The appearance of DNA in these cells was reminiscent of what is seen in *rad12*$^-$ cells upon exit from a cell cycle checkpoint-induced arrest (20,21). The chromosomal aberrations seen in *top3*$^-$ cells differ from those described in ‘cut’ mutants where abnormal chromosomal segregation arises when the septum cuts through the nucleus. In Figure 3 there are no visible septa bisecting the cells, rather, the DNA appears to be torn apart and so we propose to call this phenotype ‘torn’. Cells grown for 72 h had progressed to forming visible colonies. Microcolonies, presumed to be *top3*::*kan*^{R}, were plucked from plates and stained with DAPI. These cells had more pronounced morphological changes, with more severely fragmented chromosomes, acentric nuclei and often had DAPI stained material scattered throughout the cell (Fig. 3E–H). We cannot dismiss the possibility that some of the morphological abnormalities seen in

Table 3. Comparison of topoisomerase 3 in various organisms

Organism/gene	Identity[a]	Similarity[a]	Region of similarity (no. of amino acids)	Genbank accession no.
Saccharomyces cerevisiae TOP3	44%	60%	654	P13099
Human *TOP3*	42%	63%	600	Q13472
Mouse *TOP3*	42%	63%	598	BAA25662
Caenorhabditis elegans TOP3	40%	60%	623	AAC13567
Drosophila melanogaster TOP3	34%	53%	591	AAD13219
Arabidopsis thaliana TOP3	30%	47%	610	AAD15404
Bacillus subtilis TOP1	23%	41%	532	P39814
Escherichia coli TOP1	24%	42%	444	P06612

[a]The percentages of identity and similarity between *S.pombe* Top3 and its homolog in the corresponding organism.

these cells are simply late events occurring in dying cells. Nonetheless, these results demonstrate that cells lacking Top3 undergo aberrant chromosomal events.

Suppression of *top3*⁻ lethality

As previously reported, the slow growth of *top3* mutants in *S.cerevisiae* is suppressed by mutations in the *SGS1* gene, the homolog of *S.pombe rad12*$^+$. To investigate whether a similar relationship exists in *S.pombe*, we deleted the *top3*$^+$ gene (*top3*::*kan*^{R}) in a *rad12* mutant strain, in which the entire helicase domain and C-terminus of Rad12 were deleted (named *rad12-hd* for helicase deleted). *rad12-hd* has been previously referred to as *rad12*::*ura4*$^+$ and was made by replacing nucleotides 1360–3462 of *rad12*$^+$ with *ura4*$^+$ (21; Fig. 4A). The double mutant *rad12-hd top3*::*kan*^{R} was viable but did not grow as well as the *rad12-hd* single mutant (Fig. 5).

To ask specifically if it was the helicase activity of Rad12 that was responsible for the lethality of *top3* mutants, a point mutation in the ATP binding domain of *rad12* was made. The mutation, *rad12-K547I*, is within the helicase domain and results in an isoleucine substitution at the invariant lysine at amino acid 547 (Fig. 4A). This lysine is conserved in all of the RecQ helicases that have been sequenced and is part of the Walker A-type nucleotide binding box. This region of the helicase domain has been shown to be important for Rad12 activity as the original *rad12-502* mutation is a T→I change at position 543 (27). The *rad12-502* mutant suppresses *top3*⁻ lethality but our previous data suggested that it may retain low activity and so we chose to make the *rad12-K547I* mutation. In previous studies, this lysine was shown to be essential in the hydrolysis of ATP and substitution of this lysine abolished helicase and ATPase activity in a number of helicases, including RecQ (28–32). Substitution of arginine for this lysine allowed ATP binding but blocked hydrolysis of ATP and therefore helicase activity in *S.cerevisiae* RAD3 protein (32), demonstrating the need for a positively charged residue at this position for ATP binding. Changing this lysine to isoleucine should block ATP hydrolysis and helicase activity. Consistent with this, the *rad12-K547I* mutant grew slowly (Fig. 5), supporting the notion of deficient helicase activity. The *rad12-K547I top3*::*kan*^{R} double mutant was viable, demonstrating that the helicase activity of Rad12 causes lethality in *top3* mutants of *S.pombe*. However, this mutant had lower growth rates and reduced plating efficiency compared with the *rad12-hd top3*::*kan*^{R} double mutant (Fig. 5 and Table 4).

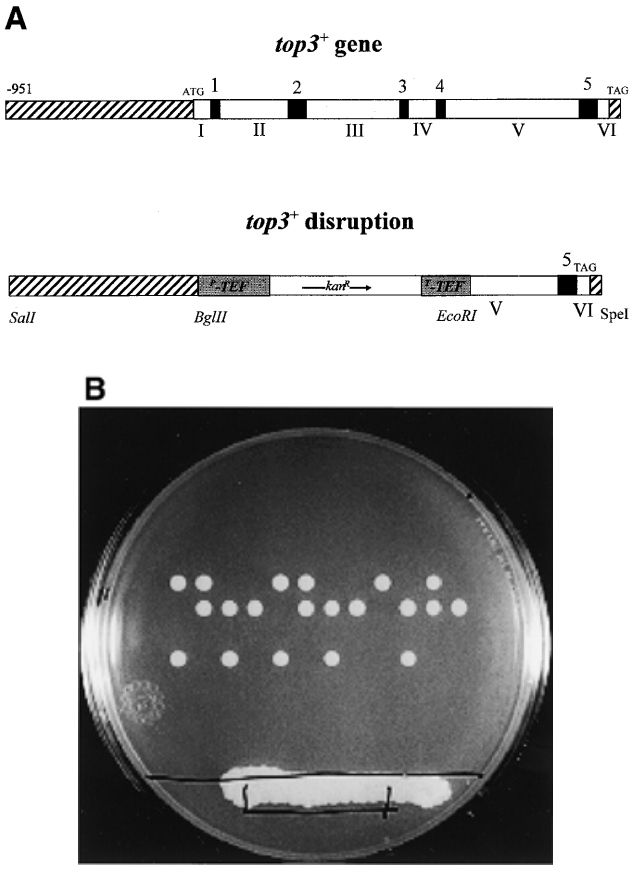

Figure 2. *top3*$^+$ is an essential gene. (**A**) PCR-generated fragments from the 5′- and 3′-ends of *top3*$^+$ were ligated onto either side of the *kan*^{r} gene within the pFA-kanMX4 plasmid creating pTop3Kmx. The disruption cassette (*top3*::*kan*^{R}) was cut out of the plasmid with *Not*I and was used to disrupt the genomic *top3*$^+$ gene in a *S.pombe* diploid strain. Black boxes represent introns (1–5), white boxes are exons (I–VI) and striped boxes show intergenic regions. The kanamycin *gene* (*kan*^{r}) is flanked by control sequences of the TEF gene (shown in gray) of the fungus *A.gossypii*. (**B**) The diploid strain was sporulated and the asci dissected. Tetrad analysis revealed a 2:0 segregation where only two spores were viable in each tetrad. Some tetrads are shown here with only one viable spore.

We then quantitated the differences in growth rates by studying growth kinetics for each single and double mutant and comparing them with the growth of wild-type *S.pombe* (972). Growth studies were carried out in three separate

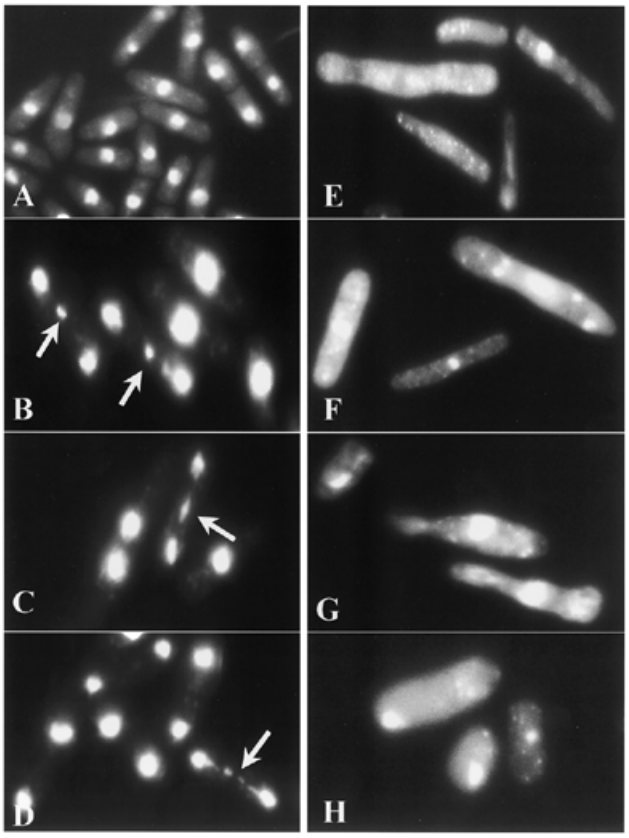

Figure 3. Fluorescence microscopic images of DAPI stained *top3*::*kan*^{R} cells. Wild-type cells are shown in (**A**). A *top3*$^+$/*top3*::*kan*^{R} strain was sporulated and treated with glusulase. Then spores were plated and allowed to grow on YEA plates. After 36 h colonies were too small to isolate individually so cells were scraped from the plates, fixed and stained with DAPI (**B**–**D**). These photographs show a mixture of *top3*$^+$ and *top3*::*kan*^{R} cells. Note the extranuclear fluorescent material and the fragmented nature of chromosomal material in the cells indicated with arrows. After 72 h microcolonies, assumed to be *top3*::*kan*^{R}, were isolated, fixed and stained (**E**–**H**). Here the cells have a much more severe phenotype, with very elongated cells and very fragmented fluorescent material. In many cells no nucleus is apparent and instead what appears to be chromosomal material is dispersed throughout the cell.

experiments where all strains were grown simultaneously. The cells were grown at 30°C in YEA with shaking. An overnight culture was grown starting with a dilution that would allow cells to reach mid-log by morning. An aliquot of cells was diluted 1:100 and counted in a Coulter counter. We carried out preliminary readings in the range of concentrations needed for these studies using the Coulter counter and showed that it gave identical cell counts to those obtained manually using a hemocytometer. Cell growth was monitored by counting cells every hour for 8 h. The data were very consistent both within and between experiments. As can be seen in Figure 5 and Table 4, both of the *rad12* single mutants grew slower than the wild-type. Of these, *rad12-hd* grew better than the point mutant *rad12-K547I*, with doubling times of 2 h 23 min and 2 h 33 min, respectively. When *top3*$^+$ was disrupted in *rad12-hd*, growth slowed only slightly (the doubling time increased from 2 h 23 min to 2 h 39 min). In contrast, growth in *rad12-K547I top3*::*kan*^{R} was severely reduced, with a doubling time of 3 h 43 min, which represents a 70 min increase in doubling time.

Fate of *top3*$^-$ cells

In addition to cell growth, we also measured cell viability. In three separate experiments cells were grown at 30°C in YEA to mid-log and counted. Based on the cell count, an aliquot of each culture was diluted and 200 cells were plated onto YEA plates. The plates were incubated for 3–5 days and counted. A summary of the results are shown in Table 4. The viability is calculated as the fraction of cells that formed colonies (i.e. no. of colonies/no. of cells plated). The average viability for wild-type cells was 90%. Each of the *rad12* single mutants showed significantly lower viability; 44% for *rad12-hd* and 18% for *rad12-K547I*. The viability decreased for each double mutant, dropping to 19% for *rad12-hd top3*::*kan*^{R} and to only 7% for *rad12-K547I top3*::*kan*^{R}. These viability results parallel the results of the growth studies, in that the viability of each strain was comparable with the growth rate. Thus, of the mutants, *rad12-hd* has the highest viability with the fastest growth rate and *rad12-K547I top3*::*kan*^{R} has the lowest viability with the slowest growth rate. What these results suggest is that the decrease in growth is not due to cells dividing more slowly, but to more cells dying.

In addition, we fixed and DAPI stained cells from each of the single and double mutants and examined them by fluorescence microscopy. Photographs of these cells are shown in Figure 6. These photographs show that in all mutant strains there is a mix of normal and elongated cells. In addition, some cells have evidence of fragmented chromosomes, revealed by multiple fluorescent spots. Chromosomal fragmentation is typically seen in elongated cells. The strains with the highest proportion of cells having altered morphologies are those with the slowest cell growth and lowest plating efficiency. Thus, comparison of *rad12-hd* with *rad12-K547I top3*::*kan*^{R} shows that *rad12-hd* has relatively few abnormal appearing cells while many *rad12-K547I top3*::*kan*^{R} cells are elongated, with smaller cells also containing some aberrant chromosomal features such as extranuclear DAPI stained material. Thus, those cells with abnormal morphologies are likely to account for the cells which are dying. There are a greater number of abnormal appearing cells in *rad12 top3* double mutants compared with *rad12* single mutants, but the abnormalities appear similar.

DISCUSSION

How do cells mutated in *top3*$^+$ die?

The findings presented here demonstrate that the *top3*$^+$ gene is essential for vegetative growth in *S.pombe*. Immediately after sporulation of a *top3*$^+$/*top3*::*kan*^{R} diploid strain, cells lacking Top3 are capable of dividing, but after a few generations cell growth stops. This would appear to be a function of accumulated chromosomal aberrations and not due to depletion of a remaining supply of active Top3 from the *top3*$^+$ allele of the diploid. This is based on observing Top3-deficient cells for 30 h after sporulation. *top3*$^+$/*top3*::*kan*^{R} diploid cells were allowed to sporulate and dissected into tetrads. Forty tetrads were followed microscopically for 30 h. What we observed was that elongated cells appeared throughout the growth of colonies, as early as the first cell division. This demonstrates that the effects of loss of Top3 on cells were immediate and not delayed, as would be expected if a supply of Top3 were being

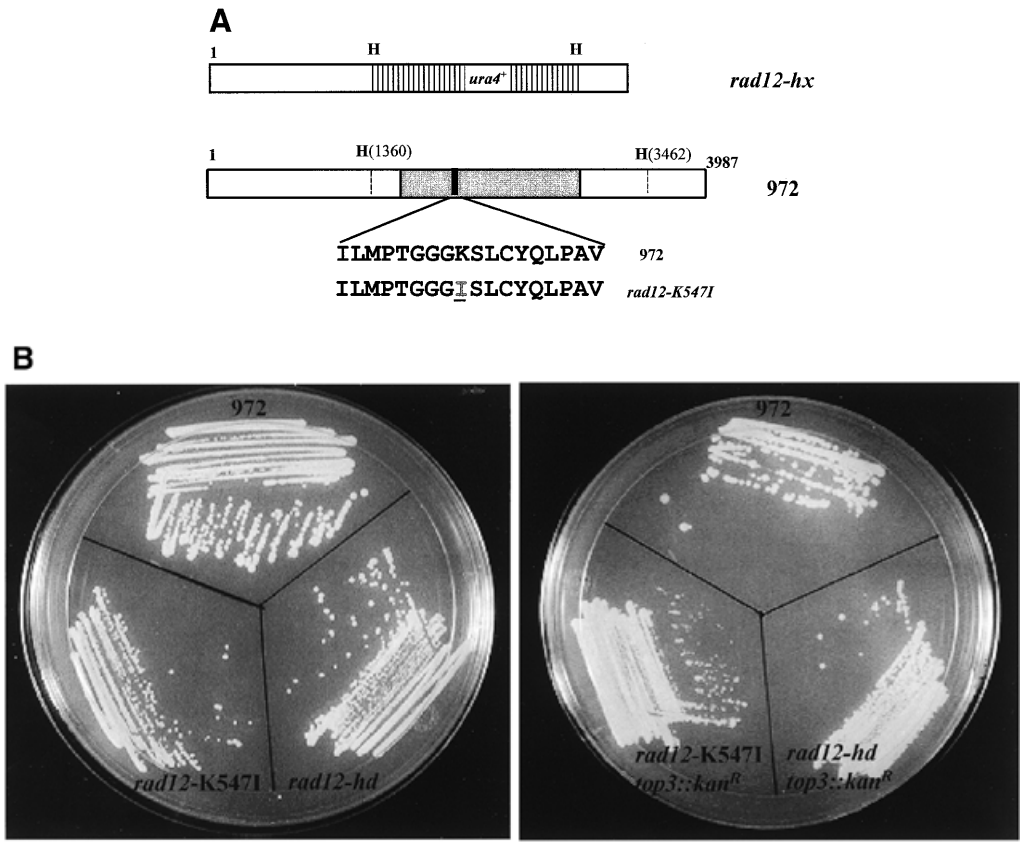

Figure 4. Mutations in *rad12*$^+$ suppress the lethality of *top3* mutations. The *top3*$^+$ gene was disrupted in two separate *rad12* mutant backgrounds, *rad12-K547I* and *rad12-hd*, to show that loss of Rad12 helicase activity restores viability in a *top3*::*kan*^{R} mutant. (**A**) Schematic of the two *rad12* mutants. The striped box indicates the *ura4*$^+$ gene within *rad12*$^+$ creating *rad12-hd*. The 2102 bp between the *Hin*dIII sites (H) were removed and the *ura4*$^+$ gene inserted on a 1.8 kb *Hin*dIII fragment. *rad12-K547I* was created by mutating the invariant lysine (K) at position 547 to an isoleucine (I). The helicase domain is indicated in gray and the Walker A-box in black. (**B**) Wild-type (972) and mutant strains were streaked onto YEA plates and incubated for 2–3 days at 30°C.

Table 4. Growth characteristics of *rad12*$^-$ and *rad12*$^-$ *top3*$^-$ mutants

Strain	Average doubling time	Growth rate relative to 972	Growth rate double/single[a]	Viability (colonies/cells plated) (range)[b]
rad12$^+$ *top3*$^+$ (972)[c]	1 h 52 min	–	–	0.897 (0.72–1.16)
rad12-hd top3$^+$	2 h 23 min	78%	–	0.312 (0.25–0.46)
rad12-hd top3::*kmx*$^+$	2 h 39 min	70%	90%	0.189 (0.08–0.25)
rad12-K547I top3$^+$	2 h 33 min	73%	–	0.18 (0.15–0.22)
rad12-K547I top3::*kmx*$^+$	3h 43 min	50%	69%	0.07 (0.05–0.08)

[a]The growth rate double/single corresponds to the growth of the double mutant *rad12*$^-$ *top3*$^-$ relative to its corresponding single mutant *rad12*$^-$.
[b]The viability (colonies/cells plated) corresponds to the plating efficiency.
[c]In this study 972 is used as the reference strain.

depleted. Also, some colonies accumulated as few as 6–20 cells where others grew to as many as several hundred before growth ceased. If active Top3 was being titrated out we would predict a more uniform number of cells to accumulate in each colony. The assumption that *top3* mutants die as a result of accumulated chromosomal aberrations is based on the observations seen in DAPI stained cells.

It was previously demonstrated that in *rad12*$^+$ mutants, chromosomal aberrations are readily visualized in cells exiting a cell cycle checkpoint arrest (20,21). These aberrations were observed in DAPI stained dividing cells, where the bulk of the DNA can typically be seen to have separated but some DNA is seen strung out between the two nuclei. This is the same appearance that DNA has in DAPI stained *top3*::*kan*^{R} cells seen in Figure 3B–D. We assume that this extranuclear DNA occurs as a result of unsegregated sister chromatids, similar to what was described in *rad12*$^+$ mutants upon exit from an induced S phase checkpoint arrest, where this was attributed to a defect in the suppression of recombination (20). In these cells there is no evidence that the septum is cleaving the nucleus.

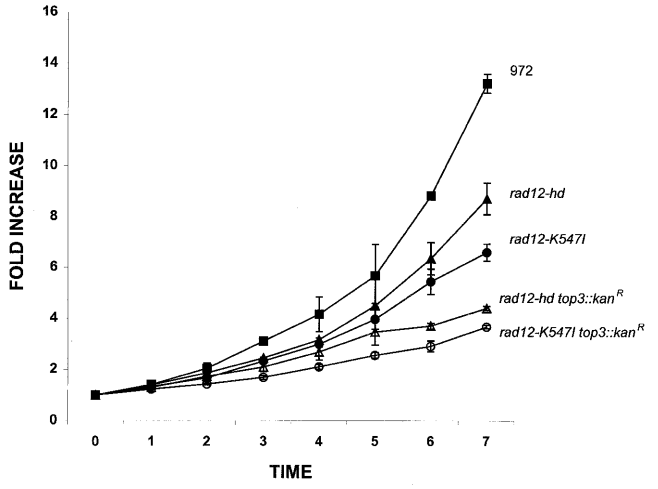

Figure 5. Growth kinetics. YEA was inoculated with each strain at a cell concentration that overnight yielded logarithmic growing cultures of similar cell concentration (0.5×10^4–2.0×10^5) the next morning. Aliquots of cell suspensions were taken every hour for 7 h and the cell count determined at each time point in a Coulter counter. The plot shows the average of three independent experiments. In some cases the error bars are smaller than the symbol and so are not visible. (Square), 972; (filled triangle), *rad12-hd*; (filled circle), *rad12-K547I*; (open triangle), *rad12-hd top3*::*kan*^{R}; (open circle), *rad12-K547I top3*::*kan*^{R}.

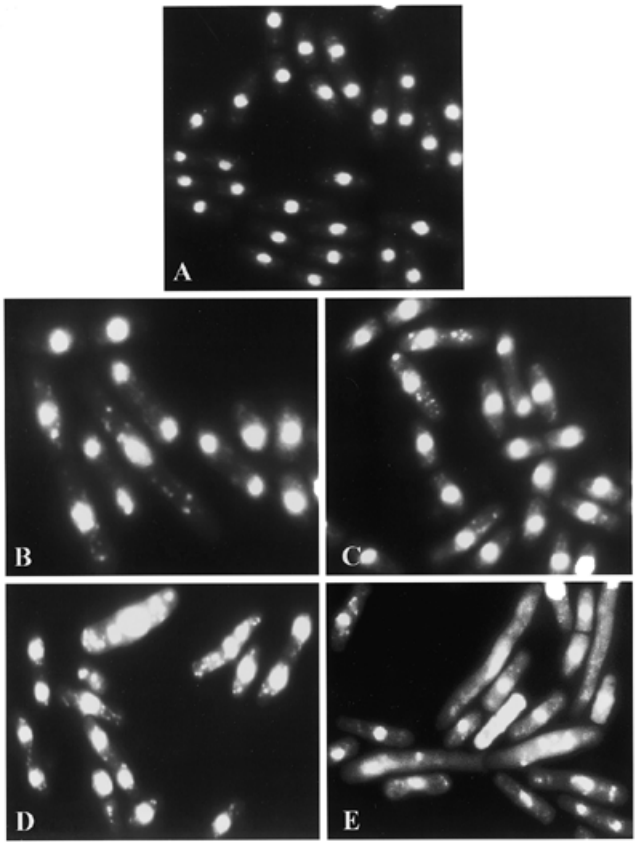

Figure 6. Fluorescence microscopy showing the morphologies of the single and double mutants. Cells were isolated, fixed and stained with DAPI from mid-log cultures of each strain. It is clear that the increased severity and frequency of nuclear abnormalities and cellular morphologies parallels the severity of the phenotype in terms of growth and viability.

We refer to this phenotype as 'torn' to distinguish it from the 'cut' phenotype that occurs in *S.pombe* cells mutated in *top2*$^+$ or in one of the *cut* genes (33–36). Microcolonies formed on plates grown for 3 days, presumed to be *top3*::*kan*^{R} were picked with the aid of a microscope. Multiple colonies were picked, stained with DAPI and examined microscopically (Fig. 3E–H). Here we see that the chromosomes appear very degraded with cells having unusual and elongated shapes. DAPI stained material is seen throughout, suggesting fragmented chromosomes. While it is likely that some portion of these alterations are attributable to loss of Top3, these cells are also dead. Therefore, we cannot rule out the possibility that some of the chaotic appearance in these cells is typical of any dying cell. Nonetheless, it would appear that in *S.pombe*, cells lacking Top3 die as the result of an inability to properly segregate their chromosomes. Finally, it is interesting to note the reduced spore viability in a *top3*$^+$/*top3*::*kan*^{R} heterozygous diploid (Fig. 2B). Comparatively, it had also been reported that null mutations of *TOP3* in *S.cerevisiae* display a pleiotropic phenotype including a sporulation defect (9).

Cell viability and growth kinetics

In this study we have used two parameters to quantitate the ability of *rad12* mutants to suppress the lethality of cells lacking Top3. Growth kinetics measure the rate of increase in cell number in a culture in log growth from which we can calculate an average doubling time. Plating efficiency is a measure of cell viability, where we plate a specific number of cells from a mid-log culture, incubate the plates for 3–5 days and count the number of colonies formed. These two measurements are not independent and in fact the slow growth in these mutants may be due to reduced cell viability. As seen in Figure 6, dividing cells in the mutant strains are similar in size to dividing wild-type cells. Since cell length is a reflection of cell division time in *S.pombe*, we conclude that these mutants have the same, or very similar, doubling times as wild-type cells.

Is it the Rad12 helicase activity that causes cell death in *top3*$^-$ cells?

Our results, showing that the lethality seen in *top3*::*kan*^{R} mutants is suppressed in a *rad12*$^-$ background, are reminiscent of the results in *S.cerevisiae* where the slow growth phenotype of a *top3* mutant is suppressed in a *sgs1* mutant background (9). These results suggest that the phenotypes associated with loss of Top3 occur because this topoisomerase is needed to resolve some intermediate that is generated by the RecQ helicase activity of Rad12 or Sgs1. This conclusion is in conflict with the results of one report in *S.cerevisiae* (37). In that study *SGS1* was mutated at the invariant lysine in the ATP binding domain within the Walker A-box which is known to completely block ATPase and helicase activity. This mutant, *sgs1-hd*, was shown to completely lack helicase activity. *sgs1-hd* was transformed into a *sgs1 top3* double mutant on a plasmid. The transformed cells were shown to behave as if they were wild-type for *SGS1*, i.e. the cells grew slowly. These data demonstrate that it is some function other than the helicase that is responsible for the suppression of Top3 activity in *S.cerevisiae*.

In our studies, we used two *rad12* mutants to suppress *top3*$^-$ lethality; *rad12-hd* has a deletion of the entire helicase domain, while *rad12-K547I* has a point mutation at the invariant lysine that should eliminate ATP binding and helicase activity (see Fig. 4A). *rad12-hd* is a null mutant eliminating the terminal two-thirds of the gene. The *top3*::*kan*^{R} mutation was introduced into each of these *rad12*$^-$ strains by gene replacement and the double mutants analyzed for viability and cell growth. Both double mutants were viable, showing that either mutation suppresses the lethal effects of deleting *top3*. The fact that a point mutation thought to inactivate the helicase activity of Rad12 suppresses loss of Top3 argues that the helicase activity is responsible for this lethality, however, the degree to which these two alleles could suppress the lethality differed greatly. In the case of *rad12-hd top3*::*kan*^{R} we found that cell viability was 19%, compared with 31% for the *rad12-hd* single mutant. The doubling time for *rad12-hd top3*::*kan*^{R} was 2 h 39 min, a 17 min decrease from the *rad12-hd* single mutant. There is a correspondingly small increase in morphological aberrations seen in the double mutant compared with the single mutant as well. In contrast, *rad12-K547I* mutants were much less efficient in suppressing the lethality of *top3*::*kan*^{R}. *rad12-K547I top3*::*kan*^{R} had greatly reduced cell viability, extremely slow cell growth and extreme morphological changes to the cells. The viability of *rad12-K547I top3*::*kan*^{R} was only 8%, with a doubling time of 3 h 43 min. The reduced viability and growth kinetics are borne out by the extreme level of morphological abnormalities seen in these double mutants (Fig. 6). It should be noted that while it is assumed that the *rad12-K547I* mutant lacks helicase activity, it is possible that low levels of activity exist and this could be the cause of the reduced viability seen in this mutant compared with the *rad12-hd* mutant.

From these results we draw three conclusions. First, the helicase is partially responsible for cell lethality in *S.pombe top3* mutants, as inactivation of the helicase partially restores viability. Second, some other activity in Rad12 also contributes to the lethality of *top3* mutants, as cell viability and growth are greatly improved when the entire Rad12 is deleted as in *rad12-hd top3*::*kan*^{R}, compared with simply inactivating the Rad12 helicase as in *rad12-K547I top3*::*kan*^{R}. This would partially support the conclusions of Lu *et al*. (37) in claiming that something other than the Sgs1 helicase causes slow growth in *S.cerevisiae top3* mutants. An alternative explanation in *S.pombe* is that inactive Rad12 binds to its target DNA but with no helicase activity to move it along, it creates a block that is unable to move along the DNA. Third, Top3 appears to have essential functions independent of Rad12 based on the fact that neither *rad12* mutant completely suppresses the lethality of *top3* mutants. This is seen by comparing growth and viability of each single *rad12* mutant with their corresponding double mutant.

Comparison of *top3* mutation in *S.pombe* and *S.cerevisiae*

The lethality seen in *S.pombe top3* mutants is in contrast to the phenotype of *S.cerevisiae top3* mutants which, despite their slow growth compared to the wild-type, are viable. This lethality appears to more closely reflect the situation in *mTOP3*α knockout mice, which die early in embryogenesis even though the mouse genome contains at least one additional *top3* homolog, *mTOP3*β (6). The lethality associated with loss of Top3 in *S.pombe* is partially suppressed by mutations in *rad12*$^+$, while in *S.cerevisiae* the slow growth of *top3* mutants is completely suppressed by mutations in *SGS1*. We would not anticipate that *rad12 top3* double mutants would grow at wild-type rates as *S.pombe rad12* single mutants already grow more slowly and have reduced viability compared with wild-type cells. However, the *rad12 top3* double mutants do not recover to the growth rates of the *rad12* single mutants. This result demonstrates that Top3 must also function independently of Rad12. This does not appear to be the case in *S.cerevisiae*. It may eventually be shown that for Rad12 it has functions that are independent of Top3.

The *rad12-hd* deletion mutant grows much better than the *rad12-K547I* point mutant. These data suggest that the presence of Rad12 with an inactivated helicase is detrimental to the cell. Results from both *S.pombe* and *S.cerevisiae* support the conclusion that most of the effects associated with loss of Top3 depend on the presence of Rad12/Sgs1. Together, our results demonstrate that Top3 and Rad12 play similar roles to their counterparts in *S.cerevisiae*, however, differences suggest that they appear to play a more complex role in *S.pombe*. While there is a large body of data concerning phenotypes associated with loss of the RecQ helicases and Topo III, the actual biological functions of these proteins remain to be determined.

NOTE

The authors note that during the time in which this work was under review a manuscript similar in scope was published in *Nucleic Acids Research* (38).

ACKNOWLEDGEMENTS

We are grateful for the assistance of Ms Eva Lin. We would also like to thank Scott Davey and Justin Weinstein for critical reading of this manuscript. This work was supported by Public Health Service grant CA-72647 from the National Cancer Institute and ES-07940 from the National Institute of Environmental Health Sciences.

REFERENCES

1. Hanai,R., Caron,P.R. and Wang,J.C. (1996) *Proc. Natl Acad. Sci. USA*, **93**, 3653–3657.
2. Seki,T., Seki,M., Katada,T. and Enomoto,T. (1998) *Biochim. Biophys. Acta*, **1396**, 127–131.
3. DiGate,R.J. and Marians,K.J. (1988) *J. Biol. Chem.*, **263**, 13366–13373.
4. Harmon,F.G., DiGate,R.J. and Kowalczykowski,S.C. (1999) *Mol. Cell*, **3**, 611–620.
5. Kim,R.A. and Wang,J.C. (1992) *J. Biol. Chem.*, **267**, 17178–17185.
6. Li,W. and Wang,J.C. (1998) *Proc. Natl Acad. Sci. USA*, **95**, 1010–1013.
7. Wallis,J.W., Chrebet,G., Brodsky,G., Rolfe,M. and Rothstein,R. (1989) *Cell*, **58**, 409–419.
8. Seki,T., Wang,W.S., Okumura,N., Seki,M., Katada,T. and Enomoto,T. (1998) *Biochim. Biophys. Acta*, **1398**, 377–381.
9. Gangloff,S., McDonald,J.P., Bendixen,C., Arthur,L. and Rothstein,R. (1994) *Mol. Cell. Biol.*, **14**, 8391–8398.
10. Watt,P.M., Louis,E.J., Borts,R.H. and Hickson,I.D. (1995) *Cell*, **81**, 253–260.
11. Hanada,K., Ukita,T., Kohno,Y., Saito,K., Kato,J. and Ikeda,H. (1997) *Proc. Natl Acad. Sci. USA*, **94**, 3860–3865.
12. Nakayama,K., Irino,N. and Nakayama,H. (1985) *Mol. Gen. Genet.*, **200**, 266–271.
13. Nakayama,K., Shiota,S. and Nakayama,H. (1988) *Can. J. Microbiol.*, **34**, 905–907.
14. Ellis,N.A., Groden,J., Ye,T.Z., Straughen,J., Lennon,D.J., Ciocci,S., Proytcheva,M. and German,J. (1995) *Cell*, **83**, 655–666.

15. Matsumoto,T., Imamura,O., Yamabe,Y., Kuromitsu,J., Tokutake,Y., Shimamoto,A., Suzuki,N., Satoh,M., Kitao,S., Ichikawa,K., Kataoka,H., Sugawara,K., Thomas,W., Mason,B., Tsuchihashi,Z., Drayna,D., Sugawara,M., Sugimoto,M., Furuichi,Y. and Goto,M. (1997) *Hum. Genet.*, **100**, 123–130.
16. Karow,J.K., Chakraverty,R.K. and Hickson,I.D. (1997) *J. Biol. Chem.*, **272**, 30611–30614.
17. Gray,M.D., Shen,J.C., Kamath-Loeb,A.S., Blank,A., Sopher,B.L., Martin,G.M., Oshima,J. and Loeb,L.A. (1997) *Nature Genet.*, **17**, 100–103.
18. Puranam,K.L. and Blackshear,P.J. (1994) *J. Biol. Chem.*, **269**, 29838–29845.
19. Kitao,S., Ohsugi,I., Ichikawa,K., Goto,M., Furuichi,Y. and Shimamoto,A. (1998) *Genomics*, **54**, 443–452.
20. Stewart,E., Chapman,C.R., Al-Khodairy,F., Carr,A.M. and Enoch,T. (1997) *EMBO J.*, **16**, 2682–2692.
21. Davey,S., Han,C.S., Ramer,S.A., Klassen,J.C., Jacobson,A., Eisenberger,A., Hopkins,K.M., Lieberman,H.B. and Freyer,G.A. (1998) *Mol. Cell. Biol.*, **18**, 2721–2728.
22. Nasim,A. and Smith,B.P. (1975) *Genetics*, **79**, 573–582.
23. Enoch,T., Carr,A.M. and Nurse,P. (1992) *Genes Dev.*, **6**, 2035–2046.
24. Freyer,G.A., Davey,S., Ferrer,J.V., Martin,A.M., Beach,D. and Doetsch,P.W. (1995) *Mol. Cell. Biol.*, **15**, 4572–4577.
25. Wach,A., Brachat,A., Pohlmann,R. and Philippsen,P. (1994) *Yeast*, **10**, 1793–1808.
26. Bahler,J., Wu,J.Q., Longtine,M.S., Shah,N.G., McKenzie,A., Steever,A.B., Wach,A., Philippsen,P. and Pringle,J.R. (1998) *Yeast*, **14**, 943–951.
27. Murray,J.M., Lindsay,H.D., Munday,C.A. and Carr,A.M. (1997) *Mol. Cell. Biol.*, **17**, 6868–6875.
28. Walker,J.E., Saraste,M., Runswick,M.J. and Gay,N.J. (1982) *EMBO J.*, **1**, 945–951.
29. Smith,R.H. and Kotin,R.M. (1998) *J. Virol.*, **72**, 4874–4881.
30. Ford,M.J., Anton,I.A. and Lane,D.P. (1988) *Nature*, **332**, 736–738.
31. Carles-Kinch,K., George,J.W. and Kreuzer,K.N. (1997) *EMBO J.*, **16**, 4142–4151.
32. Sung,P., Higgins,D., Prakash,L. and Prakash,S. (1988) *EMBO J.*, **7**, 3263–3269.
33. Uzawa,S., Samejima,I., Hirano,T., Tanaka,K. and Yanagida,M. (1990) *Cell*, **62**, 913–925.
34. Uemura,T. and Yanagida,M. (1984) *EMBO J.*, **3**, 1737–1744.
35. Uemura,T. and Yanagida,M. (1986) *EMBO J.*, **5**, 1003–1010.
36. Hirano,T., Fukahashi,S., Uemura,T. and Yanagida,M. (1986) *EMBO J.*, **5**, 2973–2979.
37. Lu,J., Mullen,J.R., Brill,S.J., Kleff,S., Romeo,A.M. and Sternglanz,R. (1996) *Nature*, **383**, 678–679.
38. Goodwin,A., Wang,S.-W, Toda,T., Norbury,C. and Hickson,I.D. (1999) *Nucleic Acids Res.*, **27**, 4050–4058.